Electronic Supplementary Information

Relations between Li+ diffusion and ion conduction for single-crystal and powder garnet-type electrolytes studied by 7Li PGSE NMR spectroscopy

Kikuko Hayamizu,[*†] Yasuhiko Terada,[†] Kunimitsu Kataoka,[‡] Junji Akimoto,[‡] and Tomoyuki Haishi[#]

[†]Institute of Applied Physics, Tsukuba University, Tennodai, Tsukuba 305-8573, Japan
[‡]National Institute of Advanced Industrial Science and Technology, AIST Tsukuba Centre 5, Tsukuba 305-8565, Japan
[#]MRTechnology Inc., Tengen, Tsukuba 300-0047, Japan

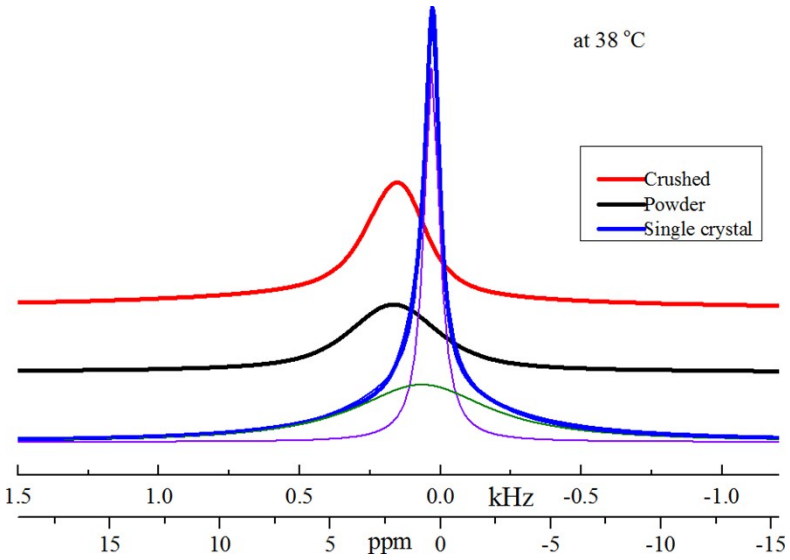

Fig. S1 ^{7}Li spectra of the single-crystal crushed and powder samples of LLZO-Nb at 38 °C. The shift positions are referred to an aqueous ^{7}Li peak. The center positions of the single crystal, crushed and powder samples were 0.39, 2.0 and 2.1 ppm, respectively at the lower field side and each spectrum is accompanied by a broad component. In the single crystal sample, decomposed two curves are shown and the position of the broad component was 0.83 ppm. The linewidths of the narrow and broad components for the single crystal were 0.066 and 0.58 kHz, respectively.

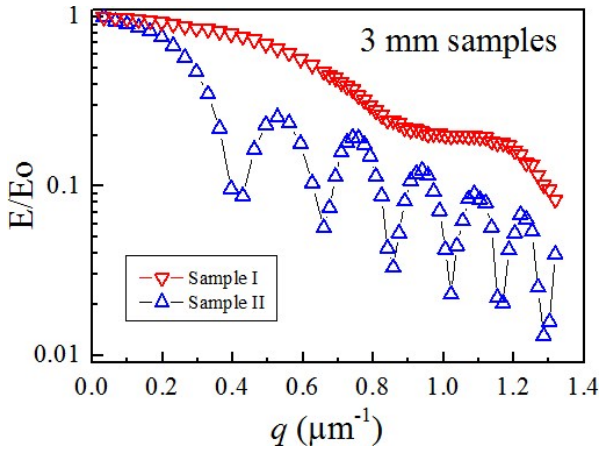

Fig. S2 Collision-diffraction patterns in echo attenuation plots for two 3 mm-high single crystal sample soon after cutting from the 6 mm-high sample. The measurement conditions were g = 10 Tm^{-1}, Δ = 10 ms, δ = 0.1 to 8.0 ms (60 points). The q values of the minimum positions were 0.41, 0.66, 0.86, 1.02, 1.17 and 1.3 μm^{-1} for the sample II.

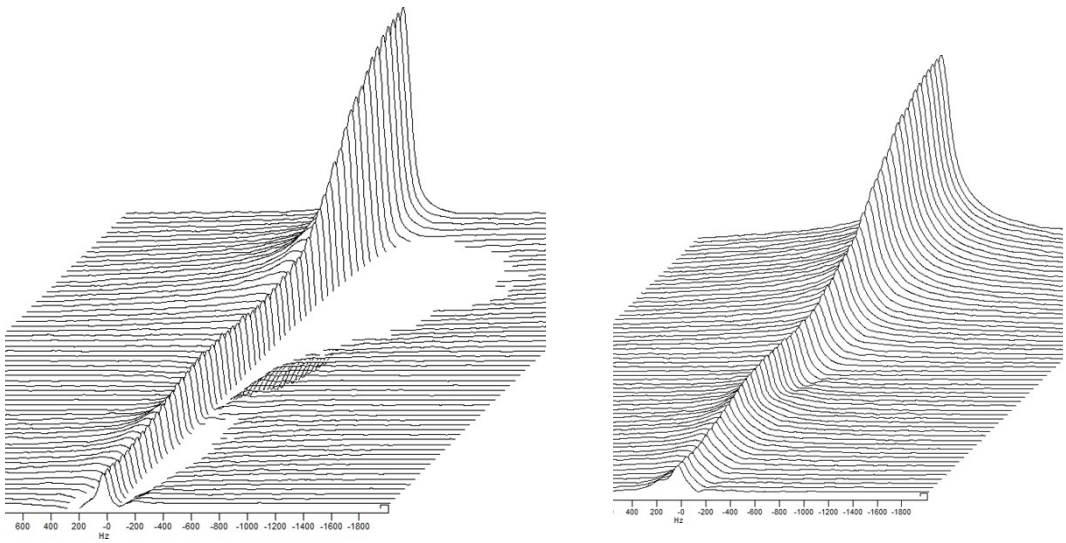

Fig. S3 Echo attenuation spectral patterns of Sample I of the 3mm-high sample of the single crystal LLZO-Nb at 65 °C, left: real mode and right: magnitude mode. Measuring conditions: Δ = 10 ms, g = 10.0 Tm^{-1}, and δ = 0.1 ~ 8.0 ms (60 points).

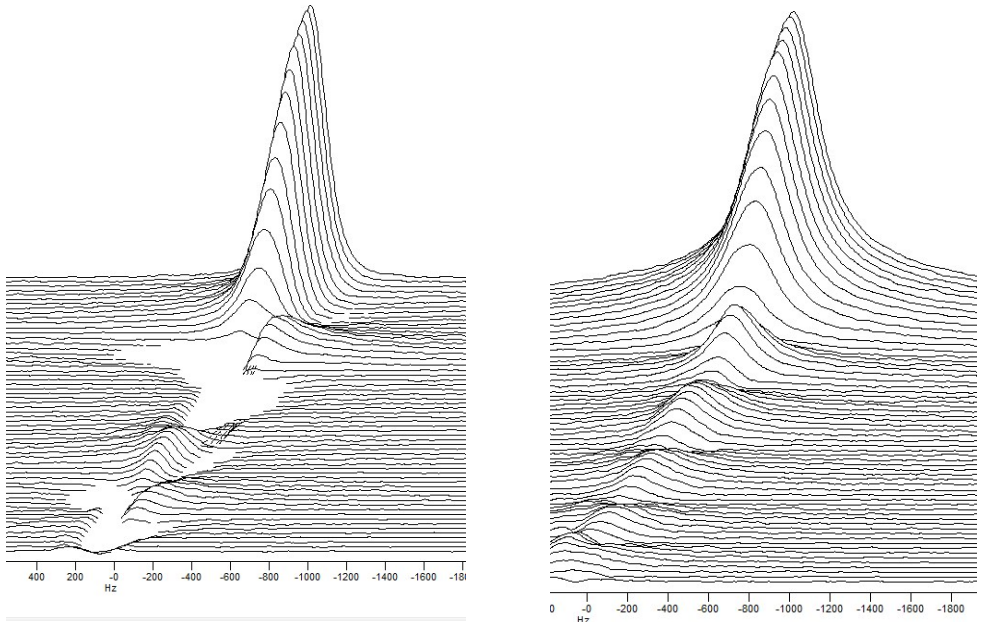

Fig. S4 Echo attenuation spectral patterns of the crushed sample of LLZO-Nb at 65 °C, left: real mode and right: magnitude mode. Measuring conditions: Δ = 10 ms, g = 10.0 Tm^{-1}, and δ = 0.1 ~ 8.0 ms (60 points). In the real mode, the phase rotations at the diffractions were observed.

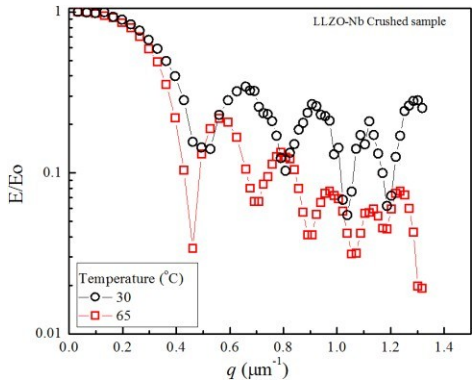

Fig. S5 Echo-attenuation plots of the crushed sample of LLZO-Nb at 30 and 65 °C. The measurement conditions were g = 10 Tm^{-1}, Δ = 10 ms, δ = 0.1 to 8.0 ms (60 points).

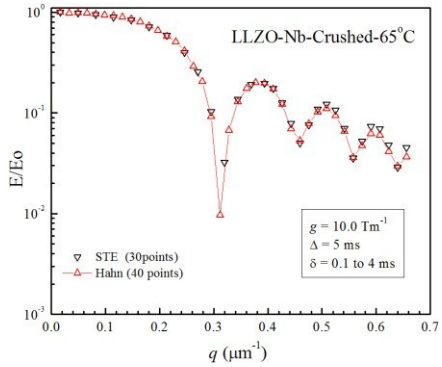

Fig. S6 The confirmation of the STE and Hahn echo sequences for the crushed sample of LLZO-Nb at 65 °C with g = 10.0 Tm^{-1}, Δ = 5 ms and δ = 0.1 to 4.0 ms.

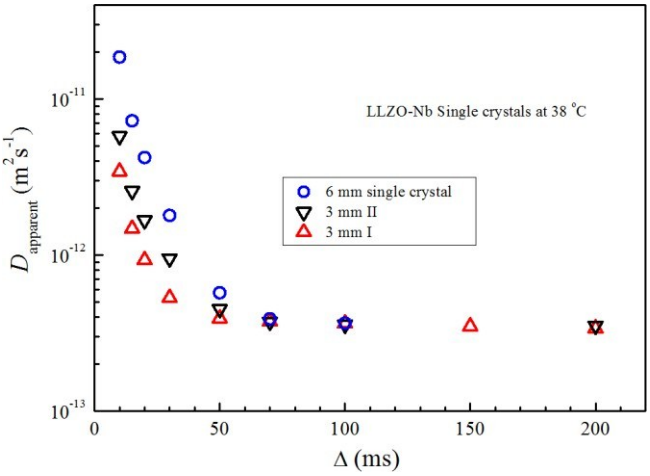

Fig. S7 Δ-dependent $D_{apparent}$ at 38 ° for the single crystal LLZO-Nb samples (6 mm, 3 mm I, and 3 mm II samples). The results of 3 mm-samples I and II were reproduced after two months.

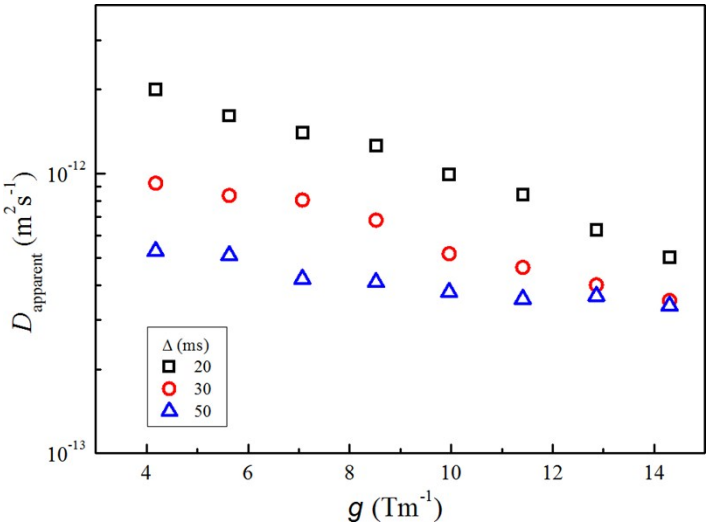

Fig. S8 g-Dependent apparent D_{Li} at 38 °C for the 3 mm-high single-crystal LLZO-Nb sample with Δ = 20, 30, and 50 ms.

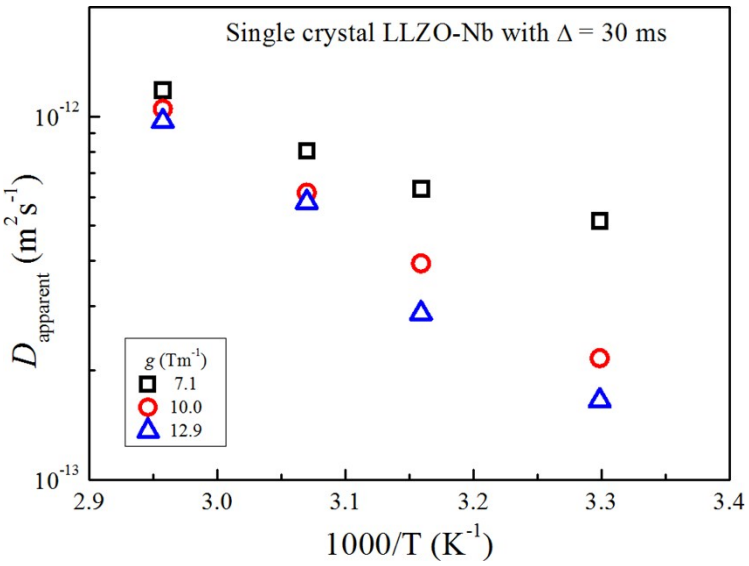

Fig. S9 Arrhenius-type plots of the $D_{apparent}$ values for 3 mm-high single crystal LLZO-Nb measured with Δ = 30 ms for g = 7.1, 10.0 and 12.9 Tm^{-1}. g-Dependent Li diffusion suggests the dispersive Li migration and smaller g value can observe faster Li diffusion. The apparent activation energy for smaller g-value seems smaller. The relative Li numbers for a different g value are unknown at each temperature.

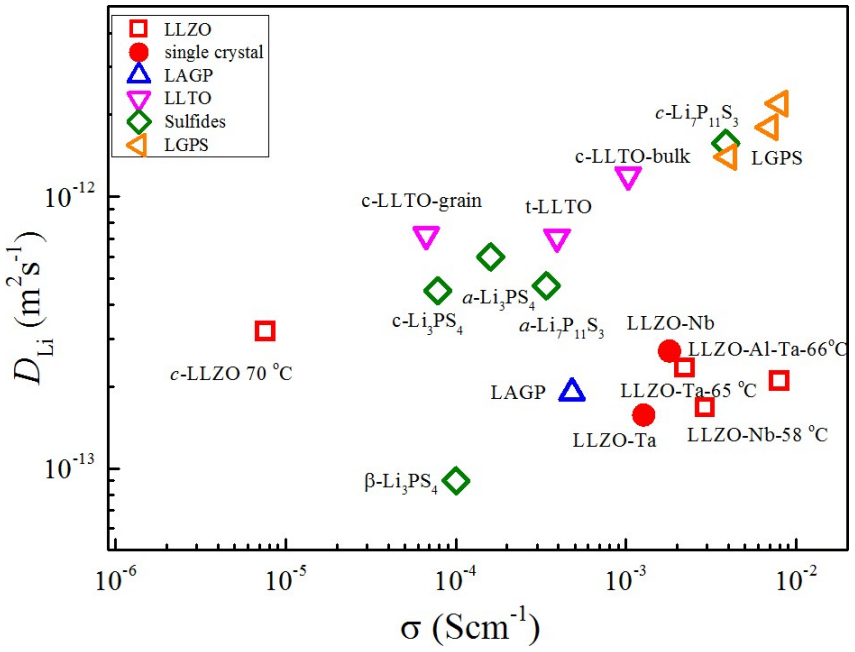

Fig. S10 D_{Li} versus σ for 17 inorganic solid electrolytes near room temperature except for four powder garnet samples. Solid marks mean single crystal samples.

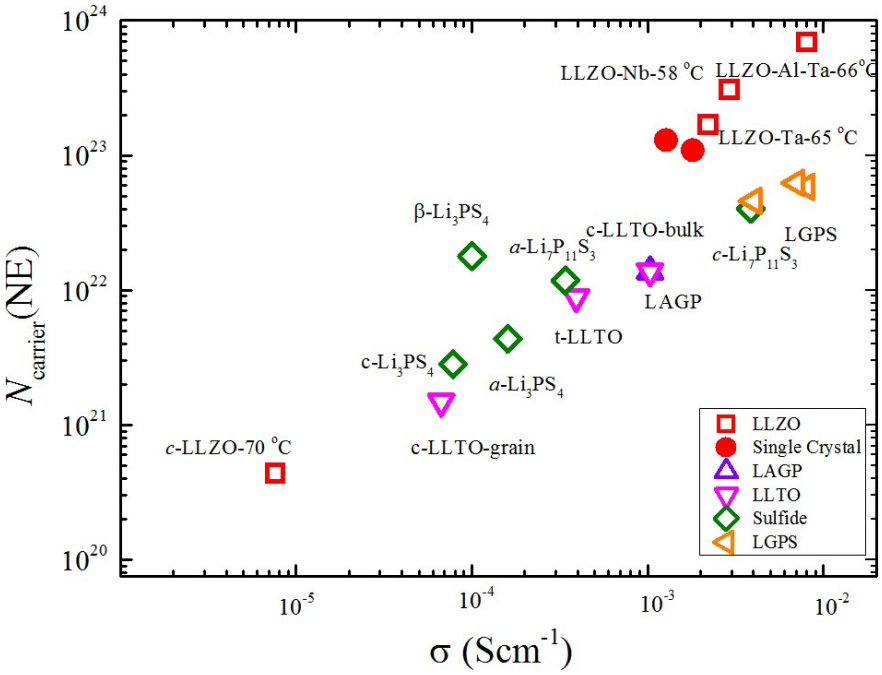

Fig. S11 N_{NE} versus σ for 13 inorganic solid electrolytes near room temperature except for four powder garnet samples at elevated temperatures. Solid marks mean single crystal samples.

Table SI. Estimated number of Li atoms in unit volume (N_{Li} cm^{-3})

Sample		MF	MW	d $g\ cm^{-3}$	N_{Li} cm^{-3}
c-LLZO	powder	$Li_7La_3Zr_2O_{12}$	839.8	5.1	$2.5_6 \times 10^{22}$
c-LLZO-Ta	single crystal	$Li_{6.5}La_3Zr_{1.5}Ta_{0.5}O_{12}$,	881.2	5.34	$2.3_7 \times 10^{22}$
	powder	$Li_{6.6}La_3Zr_{1.6}Ta_{0.4}O_{12}$	872.9	5.35	$2.4_3 \times 10^{22}$
c-LLZO-Nb	single crystal	$Li_{6.5}La_3Zr_{1.5}Nb_{0.5}O_{12}$	837.1,	5.16	$2.4_1 \times 10^{22}$
	powder	$Li_{6.75}La_3Zr_{1.5}Nb_{0.25}O_{12}$	812.2	-	
c-LLZO-Al-Ta	powder	$Li_{6.52}Al_{0.05}La_3Zr_{1.75}Ta_{0.25}O_{12}$	860.2	5.13	$2.3_4 \times 10^{22}$

Table SII. Ionic conductivity (σ) and Li diffusion (D_{Li}) for inorganic solid electrolytes

Name	**σ (Scm^{-1})**	**D_{Li} (m^{2}s^{-1})**	**N_{NE} (cm^{-3})**	**MF**	**Temp (^{o}C)**		Ref
cubic LLZO		3.2×10^{-13}		$Li_7La_3Zr_2O_{12}$	70	Powder	1
cubic LLZO	7.6×10^{-6}	3.5×10^{-13}	$4.3_8 \times 10^{20}$	$Li_7La_3Zr_2O_{12}$	70	Pellet	1, 2
cubic LLZO-Ta	1.3×10^{-3}	1.6×10^{-13}	1.3×10^{23}	$Li_{6.5}La_3Zr_{1.5}Ta_{0.5}O_{12}$	25	Single crystal	3, 4
cubic LLZO-Ta	2.2×10^{-3}	$2.3_5 \times 10^{-13}$	1.7×10^{23}	$Li_{6.6}La_3Zr_{1.6}Ta_{0.4}O_{12}$	65	powder	5, 2
cubic LLZO-Nb	1.8×10^{-3}	2.7×10^{-13}	$1.1_1 \times 10^{23}$	$Li_{6.5}La_3Zr_{1.5}Nb_{0.5}O_{12}$	32	Single crystal	6,7
cubic LLZO-Nb	2.9×10^{-3}	1.7×10^{-13}	3.1×10^{23}	$Li_{6.75}La_3Zr_{1.76}Nb_{0.25}O_{12}$	58	Powder	6, 8
Cubic LLZO-Al-Ta	8.0×10^{-3}	2.1×10^{-13}	$6.9_3 \times 10^{23}$	$Li_{6.51}Al_{0.08}La_3Zr_{1.75}Ta_{0.25}O_{12}$	66	Powder	2
LAGP	4.8×10^{-4}	1.9×10^{-13}	$4.0_6 \times 10^{22}$	$Li_{1.5}Al_{0.5}Ge_{1.5}(PO_4)_3$	25	Powder	9, 10
cubic LLTO	1.0×10^{-3}	1.2×10^{-12}	$1.3_7 \times 10^{22}$	$Li_{0.33}La_{0.55}TiO_3$	25	bulk	11,12
cubic LLTO	6.7×10^{-5}	7.2×10^{-13}	1.5×10^{21}	$Li_{0.33}La_{0.55}TiO_3$	25	grain	11, 12
tetragonal LLZO	3.9×10^{-4}	7.1×10^{-13}	8.9×10^{21}	$Li_{0.33}La_{0.55}TiO_3$	25	bulk	11, 13
Crystalline $Li_7S_{11}P_3$	$3.8_6 \times 10^{-3}$	1.6×10^{-12}	4.0×10^{22}	$(Li_2S)_7(P_2S_5)_3$	30	Powder	14
Amorphous $Li_7S_{11}P_3$	3.4×10^{-4}	4.7×10^{-13}	1.2×10^{22}	$(Li_2S)_7(P_2S_5)_3$	30	Powder	14
Crystalline Li_3PS_4	7.8×10^{-5}	4.5×10^{-13}	2.8×10^{21}	$(Li_2S)_{75}(P_2S_5)_{25}$	30	Powder	15
Amorphous Li_3PS_4	1.6×10^{-4}	6.0×10^{-13}	4.4×10^{21}	$(Li_2S)_{75}(P_2S_5)_{25}$	30	Powder	15
β-Li_3PS_4	1.0×10^{-4}	9.0×10^{-14}	1.8×10^{22}	$(Li_2S)_{75}(P_2S_5)_{25}$	25	Powder	16
LGPS	4.0×10^{-3}	1.4×10^{-12}	4.6×10^{22}	$Li_{10}SnP_2S_{12}$	room temp.	Powder	17,18
LGPS	8.0×10^{-3}	2.2×10^{-12}	5.8×10^{22}	$Li_{10}GeP_2S_{12}$	room temp.	Powder	17,18
LGPS	7.0×10^{-3}	1.8×10^{-12}	6.2×10^{22}	Li_7GePS_8	room temp.	Powder	17,18

References

1. K. Hayamizu, S. Seki, T. Haishi, *J. Chem. Phys.* 2017, **146**, 024701. (D_{Li})
2. Y. Matsuda, Y. Itami, K. Hayamizu, T. Ishigaki, M. Matsui, Y. Takeda, O. Yamamoto, N. Imanishia, *RSC Adv.*, 2016, **6**, 78210-78218. (σ)
3. K. Hayamizu, Y. Terada, K. Kataoka, J. Akimoto, *J. Chem. Phys*. 2019, **150**, 194502. (D_{Li})

4. K. Kataoka, J. Akimoto, *ChemElectroChem*, 2018, **5**, 1. (σ)
5. K. Hayamizu, Y. Matsuda, M. Matsui, N. Imanishi, *Solid State Nucl. Magn. Reson.* 2015, **70**, 21−27.
6. K. Hayamizu, Y. Terada, K. Kataoka, J. Akimoto, T. Haishi, *Phys. Chem. Chem. Phys*. 2019, **21**, (D_{Li}). this paper.
7. K. Kataoka, N. Nagata, J. Akimoto, *Sci. Rep*. 2018, **8**, 9965. (σ)
8. S. Ohta, T. Kobayashi, T. Asaoka, *J. Power Sources*, 2011, **196**, 3342. (σ)
9. K. Hayamizu, S. Seki, *Phys. Chem. Chem. Phys*. 2017, **19**, 23485-23491. (D_{Li}).
10. http://www.material-sys.com/global/76/ (HP of Toshima Manufacturing Co. Ltd.) accessed at 4th Sept. 2019. (σ)
11. K. Hayamizu, S. Seki, T. Haishi, *Solid State Ionics* 2018, **326**, 37. (D_{Li}).
12. Y. Inaguma, C. Liquan, M. Itoh, t. Nakamura, T. Uchida, H. Ikura, M. Wakihara, Solid State Comm. 86, 689 (1993). (σ)
13. X. Gao, C.A.J.Fisher, T. Kimura, Y. H. Ikuhara, A. Kuwabara, H. Morikawa, H. Oki, T. Tojigamori, K. Kohama, Y. Ikuhara, *J. Mater. Chem. A*, 2014, **2**, 843. (σ)
14. K. Hayamizu, Y. Aihara, *Solid State Ionics*, 2013, **238**, 7-14.
15. K. Hayamizu, Y. Aihara, T.Watanabe, T. Yamada, S. Ito, N. Machida, *Solid State Ionics*, 2016, **285** 51–58.
16. H. Stöffler, T. Zinkevich, M. Yavuz, A. Senyshyn, J. Kulisch, P. Hartmann,T. Adermann, S. Randau, F.H. Richter, J. Janek, S. Indris, H. Ehrenberg, *J. Phys. Chem*. C 2018, **122**, 15954-15965.
17. A. Kuhn, O. Gerbig, C. Zhu, F. Falkenberg, J. Maier, B. Lotsch, *Phys.Chem.Chem.Phys*, 2014, **16**, 14669. (D_{Li}).
18. A. Kuhn, V. Duppel, B. V. Lotsch, *Energy Environ. Sci*. , 2013, **6**, 3548. (σ)